Int. J. Therm. Sci. (1999) 38, 27–41

On the thermal compatibility of metallic pairs in rubbing applications

Hisham A. Abdel-Aal*

Department of Mechanical Engineering, The University of North Carolina at Charlotte, Charlotte, NC, 28223, USA

(Received 4 December 1997, accepted 24 June 1998)

Abstract—This paper presents a theoretical model for the prediction of the variation in heat removal during the dry sliding of metallic surfaces with the inclusion of variable thermal properties. It is shown that the temperature-induced change in the so-called 'coefficient of heat penetration' is influential in the nature of heat dissipation at the interface. This change, termed the 'matching function', is utilised to propose a possible criterion for the choice of 'thermally compatible' materials for rubbing applications. For the optimisation of thermal conditions, this criterion requires the selection of the rubbing pair, so as to maintain, in order of preference, a positive, zero, or slightly negative matching function. A preliminary study of mild steel rubbing against the same material, and against stainless steel, is presented to illustrate the relative effects of both conductivity and the matching function. It is shown that the latter provides an indication of the nature of heat removal during contact. It is proposed that this criterion may be extended to the choice of thermally efficient tribological coatings to enhance the transfer of frictional heat away from the interface. This is directly related to the design of frictional tribo-systems such as brakes and bearings. © Elsevier, Paris

thermal compatibility / matching function / flash temperature / heat penetration / penetration depth / contact efficiency

Résumé — Compatibilité thermique de surfaces métalliques utilisées en situation de frottement. Dans cette étude, un modèle théorique, incorporant des propriétés thermiques variables, prédisant les variations de transport de chaleur provoquées par le frottement à sec de surfaces métalliques, est présenté. On y démontre que la variation du «coefficient de pénétration de chaleur» provoqué par le changement de température, dépend de la nature de la dissipation de la chaleur à l'interface. Cette variation, définie comme «fonction de compatibilité», est utilisée pour définir un critère possible pour le choix de matériaux «thermiquement compatibles» pour des applications impliquant du frottement. Afin d'optimiser les conditions thermiques, la sélection de la paire des matériaux en frottement doit se faire de manière à maintenir la fonction de compatibilité, par ordre de préférence, positive, nulle ou légèrement négative. Une étude préliminaire avec de l'acier doux frottant contre un matériau similaire et de l'acier inoxydable est présentée de manière à illustrer les effets relatifs à la conductivité ainsi qu'à la fonction de compatibilité. Il est démontré que cette dernière fournit des indications quant à la nature de la dissipation de chaleur durant le frottement. Il est suggéré que ce critère pourrait être utilisé pour le choix d'un recouvrement de surface qui soit efficace pour éloigner de l'interface la chaleur créée par frottement. Cela s'applique pour la construction de systèmes à friction tels que les freins ou les roulements. © Elsevier, Paris

compatibilité thermique / fonction de compatibilité / saut de température / pénétration thermique / profondeur de pénétration / efficacité de contact

Nomenclature

A_a	area of conduction	m^2
$A_{\Re}$	real area of contact between the sliding solids	m^2
B	initial coefficient of heat penetration	$W \cdot m^{-2} \cdot s^{-1}$
P	average contact pressure	$N \cdot m^{-2}$
Q°_{diss}	rate of total heat dissipation away from the surface	$J \cdot s^{-1}$
Q°_{gen}	rate of total heat generation at the surface	$J \cdot s^{-1}$
U_{slid}	sliding speed	$m \cdot s^{-1}$
Z_p	diffusion length	m
Z_{Pmax}	depth from the surface at which a temperature rise 1 % of that at the surface is felt	m
erfc	complementary error function $\mathrm{erfc}(x) = 1 - \mathrm{erf}(x)$	

* haabdela@uncc.edu

k_o	reference thermal conductivity.....	$W \cdot m^{-1} \cdot K^{-1}$
q_a°	rate of instantaneous heat dissipation by an individual pair of contacting asperities	$J \cdot s^{-1}$
r_a	radius of the contact spot between two contacting asperities.....	m
t_c	duration of a single contact cycle	s
t_i	instant of time within the contact cycle	s

Greek symbols

Γ	individual material matching function	
Γ_{eff}	effective matching function for the rubbing pair	
Θ_b	bulk temperature rise between two asperities.....	°C
Θ_{max}	maximum potential temperature rise at the end of the contact cycle	°C
Θ_Z	temperature rise at a depth Z from the surface.....	°C
φ	slope of the heat dissipation with temperature	$W \cdot m^{-2} \cdot °C^{-1}$
α	thermal diffusivity of the material ...	$m^2 \cdot s^{-1}$
β	temperature coefficient of the thermal conductivity	K^{-1}
η_a	efficiency of an asperity pair to dissipate heat	
μ	nominal coefficient of friction	

1. INTRODUCTION

Between two sliding solids in contact, there will be a number of pairs of micro-asperity contacts, the total area of which represents the true area of contact. When an individual asperity pair starts to slide, a quantum of heat, causing a surface temperature rise, is generated. As a result, a temperature gradient normal to the contact spot will develop. Concurrently, the thermal conductivity of both materials will undergo some change (either an increase or decrease) due to the temperature rise. Continuous sliding will lead to the development of a so-called *mechanically affected layer* in which a strong temperature gradient takes place [1]. This layer will entrain a temperature distribution which induces a corresponding point-wise variation in the thermal conductivity. This leads to variation in the heat removal with respect to position from one sub-layer to another. In this way, the variation in the thermal properties of the rubbing pair assumes an important role in the dissipation of frictional heat.

Now suppose that the contact spot between any two asperities lies within a mathematically flat plane at the surface $Z = 0$ (where the axis Z points in the direction of the outward normal to the contact spot). Heat will be conducted into both solids where there exists solid-to-solid contact. That is, essentially, heat flow is initiated at this mathematical plane, i.e. at the tips of the micro-asperities. The role of the contact spot in the flow of friction heat may be viewed as analogous to the role of a valve or a gateway in fluid flow, in the sense that heat flows (penetrates) through the contact spot towards the bulk of the micro asperities (and eventually to the bulk of the rubbing solids). To utilise the thermal storage capacity of the rubbing solids, this contact spot has to maintain maximum thermal efficiency. So, at all time increments within the contact cycle, a maximum possible rate of heat flow has to be maintained. This heat flow rate, transferred by conduction according to the model used in this work, is governed explicitly by the product of the conductivity and the temperature gradient at the surface $Z = 0$, as may be inferred from Fourier's law. In this way, the variation in the conductivity with temperature assumes an important role in maintaining the thermal efficiency of the contact spot (or the gateway in the fluid analogy). It is recognised that the thermal effusivity of the rubbing materials and its respective variation with temperature may affect heat conduction away from the contact spot. However, for the materials used in this investigation and the temperatures encountered for practical sliding systems, the variation in the effusivity with temperature is considered immaterial (see appendix).

Variation in the thermal conductivity may be classified into three broad categories according to the change in the conductivity with temperature; these are summarised in *table I*. Based on this classification we may conceive the following scenario. A *class a* material is rubbing against another *class* a material under sliding conditions that result in a high temperature rise. When the materials start to heat at the points of true contact, the conductivity will drop significantly. Meanwhile, heat continues to be generated at the interface due to continuous rubbing. As the temperatures increase, the ability of the contact spot, on both surfaces, to maintain the optimum rate of heat flow will decrease. Now if the rate of heat generation at the interface is greater than the rate of heat penetration through the micro-roughness, heat will accumulate at the interface. This heat will further raise the interfacial

TABLE I
Classification of materials according to the variation in their thermal conductivity with temperature.

Material class	Conductivity behaviour with temperature
Class a	Conductivity drops with temperature elevation (e.g., carbon steels, sapphire, and zirconium)
Class b	Conductivity increases with temperature elevation (e.g., stainless steels, duralumin, and cast iron)
Class c	The temperature–conductivity curve includes an inflation point; that is, the conductivity of the material increases (or drops) with temperature, reaches a maximum (or a minimum), then drops (or increases); (e.g., titanium, zinc and vanadium)

temperature causing a further drop in the conductivity and rendering the heat removal less efficient. If such a situation prevails for a sufficiently long time, thermal failure of the rubbing pair becomes imminent. For this reason, it is important to address the fundamental question of how to quantify and control the difference between the generated and the dissipated heat, where we understand *dissipated heat* to mean the heat which penetrates through the contact spot into both rubbing members. Perhaps more importantly, how should the designer, who is frequently faced with a situation where pre-set operation parameters are imposed, choose the materials of rubbing members so as to eliminate this difference or confine it to an absolute minimum?

In this paper the fundamental semi-infinite body solution [2] is used to identify a characteristic temperature–penetration depth which defines the extent of the temperature effects in the bulk of the material. By expressing heat dissipation in terms of the penetration depth, two fundamental quantities are identified. The first is termed *specific contact efficiency*, which represents an upper bound for the capability of a single contacting asperity pair to dissipate an applied thermal load. The second, termed *the matching function*, represents the change in the so-called *coefficient of heat penetration* [3] (or thermal effusivity). This relates the change of the thermal conductivity with temperature to the diffusivity of the material and may be used to predict the nature of heat removal with temperature rise and thereby the thermal compatibility of two materials. A criterion for the thermal compatibility of two rubbing materials, based on the value of the matching function, is proposed. The criterion requires the selection of the rubbing pair, so as to maintain, in order of preference, a positive, zero, or slightly negative matching function. The matching process is demonstrated by studying the heat removal for two rubbing pairs (mild steel (*AISI 1020*)-mild steel, and mild steel-stainless steel (*AISI 304 HN*)). It is to be noted, however, that the scope of this work does not extend to the treatment of the manner in which friction-induced heat is divided between the rubbing members.

2. THERMAL ANALYSIS

Two conforming rough solids will establish true contact between a finite number of pairs of contacting asperities. The asperity pair may be sufficiently modelled as a pair of spherically capped protrusions which, if plotted on a one-to-one scale, would resemble two semi-infinite bodies with a circular contact spot between them [4]. The model of heat transfer adopted in the current work follows that of Dundurs and Panek [5], in which the following assumptions are made: heat transfers only where there is metal-to-metal contact (i.e. at the contacting asperities only); the effects of radiation and the effects of an intervening fluid are insignificant; and there is no resistance due to an oxide film or other contamination of the surfaces.

Consider a system of two contacting asperities sliding relative to each other (*figure 1*). Choose a point located at the centre of the moving contact spot (point g in *figure 1*). The point will slide towards the leading edge of the mating asperity, point A, at time $t = 0^+$ (say). The point will continue to slide across the contact spot until it reaches a point, B, located at the trailing edge of the spot, at time $t = t_c$. It thus concludes a single rub (or a single contact cycle) in which a distance, AB, equal to the diameter of the contact spot, is covered in a time t_c. When the point moves with a uniform speed U_{slid}, the duration of a single contact cycle is defined as:

$$t_c = \frac{2r_a}{U_{slid}} \qquad (1)$$

To trace the thermal history of point g, it is necessary to divide the time of contact into j equal time increments, so that the temperature of point g at any moment within the contact cycle is a function of the temperature rise at previous times:

$$\Theta_g(t) = \sum_0^i \Theta_g(t_i) \qquad (i = 1,2,3,4,\ldots,j) \qquad (2)$$

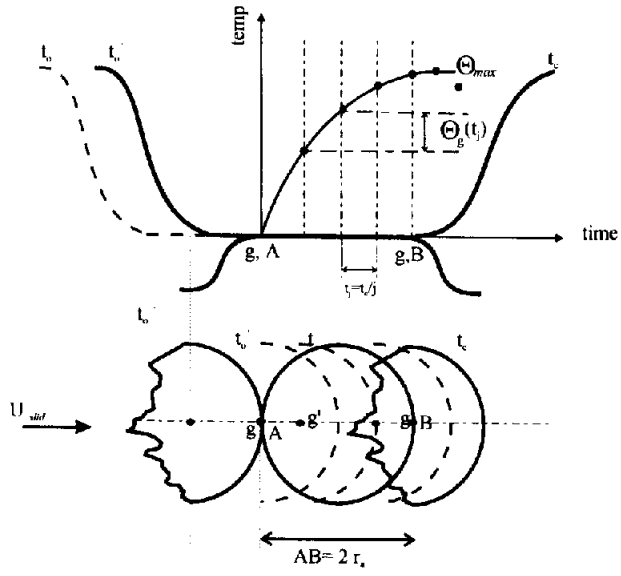

Figure 1. Schematic showing key variables of the model of contact used in the present work. Point g, located at the centre of the moving contact, slides with a uniform velocity, U_{slid}. The point approaches the leading edge of the stationary asperity, point A, then continues to slide until it reaches the trailing edge, point B. The duration of motion is t_c, in which point g covers a distance AB equal to the diameter of the contact spot. Concurrently, the temperature of the point $\Theta_g(t_i)$ increases as a function of time.

Note that, according to equation (2), the maximum temperature rise of the point will be reached at t_c where the contact spot has covered a distance equal to its diameter. At each time increment, a temperature gradient will form in each of the rubbing asperities, rising towards the contact spot, and causing heat to flow towards the bulk of the materials. Due to the temperature rise, however, the thermal conductivity of both materials will vary and hence the product of the conductivity and the temperature gradient will change accordingly. Applying Fourier's law of conduction, and assuming that the conductivity of both mating materials varies linearly with temperature, the heat conducted away from the contact spot assumes the form (see appendix 1):

$$\dot{q}_a = q_a(t_i) = \left[k_{0_1}(1+\beta_1\,\Theta_g)\left\{\frac{\Theta_g-\Theta_b}{Z_P}\right\}_1 + k_{0_2}(1+\beta_2\,\Theta_g)\left\{\frac{\Theta_g-\Theta_b}{Z_P}\right\}_2\right]^{(t_i)} A_a \quad (3)$$

Equation (3) may be extended to represent the amount of heat dissipated by n contacting asperity pairs, by summing the individual contributions of all the contacting asperity pairs. Whence it follows that the total heat dissipated through the surface per unit time is:

$$Q_{diss}(t_i) = \dot{Q}_{diss} \approx n\, q_a(t_i) \quad (4)$$

However, the total heat generated at the contact interface between the two solids is:

$$Q_{gen}(t_i) = \dot{Q}_{gen} = \mu\, P\, U_{slid}\, A_{\Re} \quad (5)$$

where P is conventionally considered as the hardness of the softest of the contacting pair for plastic contact conditions or the Hertzian contact stress for elastic contact conditions [6], and μ is the nominal coefficient of friction. Note that equation (3) may be interpreted as an upper bound to the capability of a contacting asperity pair to dissipate a thermal load (given by equation (5)) applied at the interface.

3. HEAT DISSIPATION EFFICIENCY

The maximum thermal load that can be handled in a given sliding situation is proportional to the maximum heat dissipation capacity of a contacting asperity pair. Thus, the ratio of the maximum load to the actual total thermal load applied at the interface may be read as constituting a measure of a *specific heat dissipation efficiency* (η_a) of the asperity pair defined as:

$$\eta_a = \frac{\dot{q}_a}{\dot{Q}_{gen}} \qquad (0 < \eta_a < 1) \quad (6)$$

The non-dimensional parameter η_a may also be viewed as the thermal loading limit of an asperity pair, and thus indicates the portion of the interfacial thermal load shared by an asperity pair during rubbing. The higher this parameter, the higher the ability of the solid to withstand friction induced thermal loads.

The influence of the asperities is not explicitly apparent in the model due to the definition of thermal efficiency used to develop equation (6). This efficiency is taken to indicate the ratio of the rate of heat penetration through the contact spot-between two micro asperities $q(t_i)$ to the rate of *total* heat generation at the interface Q°_{tot} (equation (5)). On balance, the influence of the number of contacts on heat sharing may be explicitly deduced if the contact efficiency is, alternatively, defined as the ratio of the rate of heat penetration through the contact spot $q(t_i)$ to the rate of heat generation at the asperity tip, i.e. $Q^{\circ}_{tot}\, n^{-m}$, where the factor m assumes the values of 1/2 or 1/4, depending on the spacing between the micro-contacts [7]. In any case, incorporating the effect of the number of micro-contacts would not affect the fundamental trends of heat penetration.

4. THE PENETRATION DEPTH OF A TEMPERATURE PULSE

Consider the semi-infinite plane shown in *figure 2*. The material and its surface are at some given initial temperature, Θ_0. At the time $t+0$ the surface is set to a temperature $\Theta_s(t)$, where $t \le t_c$. Now, define a normalised temperature $\overline{\Theta}$ that represents the ratio of the temperature rise at a depth Z, to the surface temperature, so that:

$$\overline{\Theta}(t) = \frac{\Theta_z(t)}{\Theta_s(t)} \quad (7)$$

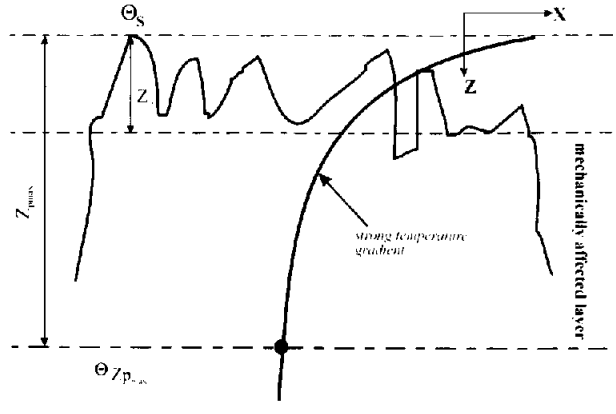

Figure 2. Schematic illustrating the development of a strong temperature gradient in the mechanically affected layer. The maximum penetration depth $Z_{p_{max}}$ is that depth at which a temperature rise amounting to 1 % of that at the surface is felt.

The temperature field in the material is given by:

$$\frac{\partial \Theta}{\partial t} = \alpha \frac{\partial^2 \Theta}{\partial Z^2} \tag{8}$$

with the boundary conditions:

$$\begin{aligned} \overline{\Theta} &= 0 \qquad t < 0, \quad 0 < z < \infty \\ \overline{\Theta} &= 1 \qquad t > 0, \quad z = 0 \end{aligned} \tag{9}$$

The solution to this problem is [1, 2]:

$$\overline{\Theta} = \frac{2}{\sqrt{\pi}} \int_{\xi}^{\infty} \exp\left\{-\xi^2\right\} \mathrm{d}\xi = \mathrm{erfc}(\xi) \tag{10}$$

where:

$$\xi = \frac{Z}{2\sqrt{\alpha t}} \tag{11}$$

The solution, equation (10), may be regarded as the response of the material to a surface temperature pulse, where the maximum response corresponds to $\Theta = 1$, while no response corresponds to $\overline{\Theta} = 0$, i.e., $0 < \Theta_{\mathrm{p}} < 1$. The equation

$$\overline{\Theta}_{\mathrm{p}} = \frac{2}{\sqrt{\pi}} \int_{\xi_{\mathrm{p}}}^{\infty} \exp\left\{-\xi^2\right\} \mathrm{d}\xi = \mathrm{erfc}(\xi_{\mathrm{p}}) \tag{12}$$

has the solution (ξ_{p}), unique to a particular Θ_{p}, such that:

$$Z_{\mathrm{p}} = 2\,\xi_{\mathrm{p}} \sqrt{\alpha t} \tag{13}$$

which is defined as the penetration depth of Θ_{p}. It follows that a unit temperature pulse on the surface causes a temperature rise of at least Θ_{p} to penetrate to a depth Z_{p}. As an example, $\Theta_{\mathrm{p}} = 0.7$ (a rise of at least 70 percent of the original pulse) is felt at a depth of:

$$Z_{0.7} = 0.275 \times 2\sqrt{\alpha t} \tag{14}$$

(using $\mathrm{erfc}(0.275) = 0.7$).

In this work, the maximum penetration depth will be considered as the depth at which a temperature rise of about 1 percent of that at the surface temperature rise is located, i.e. $Z_{0.01}$. Using $\mathrm{erfc}(2) \approx 0.01$, this depth is given by:

$$Z_{\mathrm{p_{max}}} = Z_{0.01} \simeq 4\sqrt{\alpha t} \tag{15}$$

The penetration depth given by equation (15) represents a higher bound. This is because the temperature pulse applied to the surface of the asperity flows originally in a one- dimensional manner along the Z axis until it reaches the bulk of the material, where it can travel in two or three dimensions.

5. VARIATION OF HEAT DISSIPATION WITH SURFACE TEMPERATURE RISE

Substituting equation (15) in equation (3), q° may be expressed as:

$$\dot{q}_{\mathrm{a}} = \left[k_{0_1}(1+\beta_1\,\Theta_{\mathrm{g}})\left\{\frac{\Theta_{\mathrm{g}} - \Theta_{\mathrm{b}}}{4\sqrt{\alpha_1 t}}\right\}_1 + k_{0_2}(1+\beta_2\,\Theta_{\mathrm{g}})\left\{\frac{\Theta_{\mathrm{g}} - \Theta_{\mathrm{b}}}{4\sqrt{\alpha_2 t}}\right\}_2\right] A_{\mathrm{a}} \tag{16}$$

Differentiating equation (16) with respect to the maximum temperature rise at the surface, the variation Θ_{s}, in q° per degree surface temperature rise, assumes the form:

$$\frac{\partial \dot{q}_{\mathrm{a}}}{\partial \Theta_{\mathrm{s}}} \Big/ A_{\mathrm{a}} = k_{0_1}\left[\frac{(2\,\Theta_{\mathrm{s}} - \Theta_{\mathrm{b}_1})\beta_1 + 1}{4\sqrt{\alpha_1 t}}\right] + k_{0_2}\left[\frac{(2\,\Theta_{\mathrm{s}} - \Theta_{\mathrm{b}_2})\beta_2 + 1}{4\sqrt{\alpha_2 t}}\right] = \frac{1}{4\sqrt{t}}\,\varphi \tag{17}$$

The parameter φ, which has the units of $\mathrm{W{\cdot}m^{-2}{\cdot}K^{-1}}$, incorporates the changes in the flux permitted through the asperity contact per unit area per unit surface temperature rise, or the change in the so-called *coefficient of heat penetration* per unit temperature rise. To investigate the influence of this parameter on sliding, let us assume for convenience that the surface temperature rise is considerably higher than the bulk temperature rise, i.e. $\Theta_{\mathrm{s}} \ggg \Theta_{\mathrm{b}}$. This assumption is equivalent to stating that the penetration depth of a temperature pulse extends to the location on the Z axis where no temperature rise is experienced. Under these conditions the variable φ becomes:

$$\varphi = 2\Theta_{\mathrm{s}}\left[\frac{k_{0_1}\,\beta_1}{\sqrt{\alpha_1}} + \frac{k_{0_2}\,\beta_2}{\sqrt{\alpha_2}}\right] + \left[\frac{k_{0_1}}{\sqrt{\alpha_1}} + \frac{k_{0_2}}{\sqrt{\alpha_2}}\right] \tag{18a}$$

$$\varphi = \Gamma_1(\Theta_{\mathrm{s}}) + \Gamma_2(\Theta_{\mathrm{s}}) + B = \Gamma_{\mathrm{eff}}(\Theta_{\mathrm{s}}) + B \tag{18b}$$

The parameter φ represents the slope of the heat dissipation with temperature. The sign of this quantity is an indicator of the change in heat removal with temperature rise. It will be noticed from equation (18b) that φ is composed of two competing quantities, both of which are material properties. The first, B, is a positive constant, whereas, the second, Γ_{eff}, is a linear function of the surface temperature rise representing the temperature rise-induced perturbation in the coefficient of heat penetration. This is closely related to the change in the rate of heat conducted through a contacting asperity pair.

Depending on the material class (as introduced in *table I*), Γ_{eff} may assume a positive or a negative sign. While the positive sign is desirable, a negative Γ_{eff} is

not favoured as it indicates a drop in the amount of heat conducted as the surface temperature increases. This situation takes place when a negative Γ_{eff} is greater than B so that it dominates the heat conduction process. In this case, φ will acquire a negative sign also. The ratio Γ_{eff}/B for several materials sliding against mild steel (*AISI 1020*), evaluated as a function of the surface temperature rise, is plotted in *figure 3*. Note that the effect of Γ_{eff} is more pronounced for *class a* materials (negative β coefficients), especially at higher temperatures, so the sign of φ will be determined mainly by the sign of Γ_{eff}. The function Γ_{eff} may be used to characterise the thermal compatibility of two contacting materials.

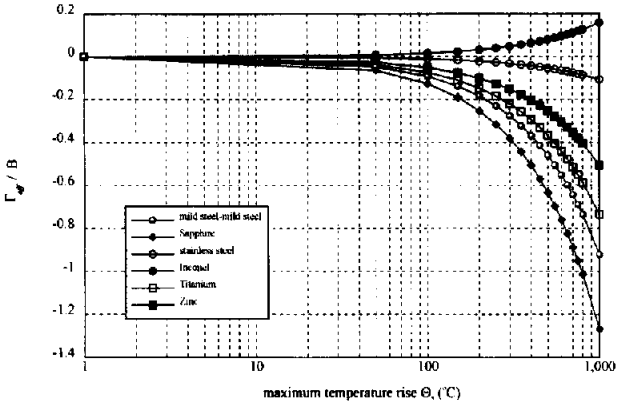

Figure 3. The variation in the ratio of the effective matching function Γ_{eff} to the room temperature coefficient of heat penetration, B, with temperature rise. All materials are sliding against mild steel (*AISI 1020*). Load = 20 N, $U_{\text{slid}} = 2\ \text{m}\cdot\text{s}^{-1}$.

The sign of the function $\Gamma(\Theta_s)$ determines the nature of heat removal away from the surface in a given contact cycle. If this function is positive, the amount of heat conducted away from the contact spot will increase with temperature elevation, thus inhibiting the conditions for thermal damage. In contrast, if this function is negative, it indicates that the amount of heat conducted away from the contact spot will decrease with temperature elevation, thereby catalysing the conditions of interfacial thermal damage. In this way, the function Γ_{eff} may be used to characterise the thermal compatibility of two rubbing materials. In this paper, this function will be termed henceforth the matching function. The criterion for thermal compatibility would thus be defined as follows: given a material for a rubbing application, what is the mating material that would insure, if possible, a positive matching function. Clearly this is not always possible, because other design constraints have to be considered too. So the next desirable condition would be to keep the matching function at zero (implying a constant heat dissipation rate for the duration of the contact cycle); or to achieve the minimum possible negative value of the matching functions (implying the minimal rate of change of heat dissipation per contact cycle).

The main influence in equation (18-b) is the constant quantity $\Gamma = k_0 \beta \alpha^{-1/2}$. The sign of this quantity follows the sign of the temperature coefficient of conductivity β. This in turn depends on the material class [8]. For *class a* materials, the β coefficient is negative; for *class b* materials, this coefficient is positive. For *class c* materials, however, the sign of the β coefficient alternates as a function of the inflation temperature. So that the conductivity variation of such materials may be best modelled by two β coefficients, as explained elsewhere [9].

For a given sliding pair, the ratio Γ_1/Γ_2 assumes considerable importance when φ is negative as it indicates which of the mating materials is more likely to dominate the heat removal process by bearing a higher portion of the friction-induced thermal load. This ratio is given in *table II* for the materials of *figure 3* under the same sliding conditions. All materials are sliding against mild steel. Notice that a positive Γ_1/Γ_2 in *table I* indicates the sliding of two *class a* materials (i.e. two negative β coefficients). It may be noticed that *class b* materials are less dominated by mild steel (compare the values of titanium and tool steel to those of Inconel and stainless steel for example).

TABLE II
Ratio of the individual matching functions Γ_1/Γ_2 for several materials sliding against mild steel (*AISI 1020*).

Material	class	Γ_1/Γ_2
Titanium	a–c	6.2764
Tool steel (*AISI 52100*)	a–a	2.098
Stainless steel (*AISI 304 HN*)	a–b	−1.31
Zinc	a–c	0.5794
Inconel	a–b	−0.7378
Mild steel (*AISI 1020*)	a–a	1

6. RESULTS AND DISCUSSION

6.1. Kinetics of the temperature gradient

Figures 4 and *5* illustrate the evolution of the temperature gradient for a stainless steel-mild steel rubbing pair. The pair is sliding at a speed of $2\ \text{m}\cdot\text{s}^{-1}$, under a nominal load of 20 N, leading to a contact radius of about 20 μm. Notice that there are several factors which act simultaneously to affect the evolution of the temperature gradient. *Figure 4* depicts the ratio of the instantaneous temperature rise to the maximum potential temperature rise at the centre of the contact spot plotted against the time of contact.

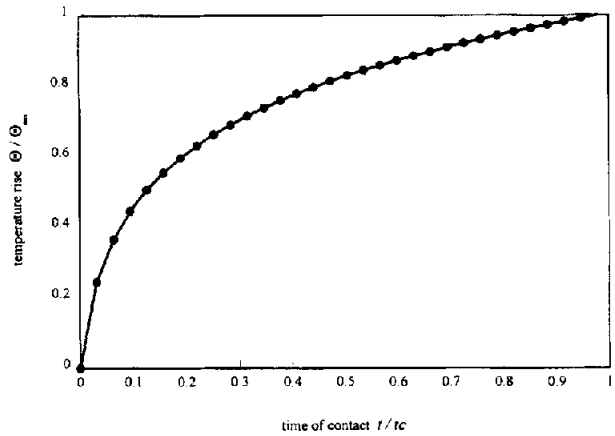

Figure 4. Variation in the instantaneous to the maximum expected temperature rise, with respect to the non-dimensional time of contact t/t_c. Temperatures were evaluated using a variable conductivity solution [7]. Mild steel (*AISI 1020*) rubbing against stainless steel (*AISI 304 HN*). Load = 30 N, $U_{slid} = 2$ m·s^{-1}.

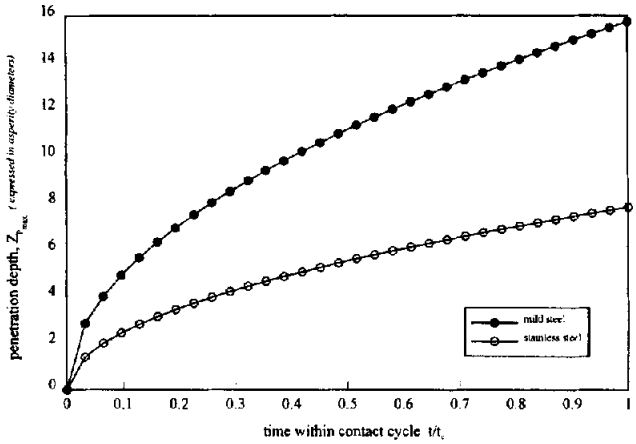

Figure 5. Variation in the penetration depth Z_{pmax} with the non-dimensional contact time t/t_c, for the rubbing pair of *figure 4*.

Notice that the rate of temperature increase (slope of the curve) decreases with time. So the contact centre experiences approximately one half of the maximum potential rise approximately in the first 15 to 20 % of the duration of contact. This temperature rise, however, is not associated with a matching growth in the penetration depth shown in *figure 5*: for the same duration of rubbing, the temperature penetrates only to an approximate one third of the maximum potential penetration depth. This results in the temperature gradient reaching a maximum early in the rubbing cycle. Consequently, the capacity of the asperity pair to dissipate heat would also reach a maximum. So the efficiency η_a is expected to peak early in the cycle. Subsequent to this maximum, the rate of temperature rise is lower than that at the beginning of the cycle. Heat pulses however penetrate to a greater depth. That is, the value $Z_{p_{max}}$ increases faster than the temperature increases (*figure 5*). So the temperature gradient (temperature difference/penetration depth) will drop accordingly. In other words, as the temperature gradient drops, the potential that drives the flow of heat will be minimised, so that unless this drop is compensated by an increase in the conductivity, the amount of heat removed away from the surface will reduce accordingly.

6.2. Effect of temperature rise on the matching function

The values of the matching function Γ_{eff} for different materials rubbing against mild steel *AISI 1020* are summarised in *table II*. It will be noticed that *class b* materials (stainless steel, and Inconel) provide a better thermal match than *class a* materials. This is due to the fact that the former have a positive Γ which delays the sharp drop in the rate of heat dissipation from the surface with temperature rise often displayed by *class a* materials. Note that as the value of the β coefficient increases the value of the matching function increases accordingly. So a material such as Inconel which has a β coefficient of around 0.002 yields the highest positive Γ value, whereas for a mild steel pair ($\beta = -0.000874$) the lowest value of Γ is obtained (≈ -8). This implies that thermal failure is more likely to occur, due to the drastic reduction in the capacity of heat removal expected at higher temperatures. This effect is best illustrated in *figure 6*, which depicts the variation in the matching function with temperature. Notice the drop in the matching function (which implies a corresponding

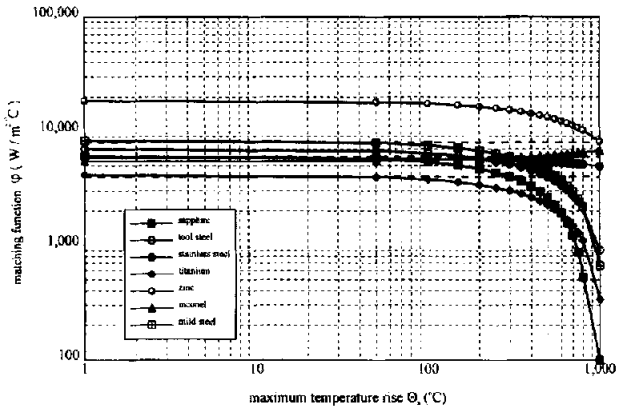

Figure 6. Variation in the matching function φ with temperature for several materials sliding against mild steel (*AISI 1020*). Load = 20 N, $U_{slid} = 2$ m·s^{-1}.

drop in the capacity for heat removal) displayed by *class a* materials (sapphire and tool steel). The capacity of heat removal is closely related to the β coefficient and the Γ values given in *table I* (compare the β values to the corresponding curves). Moreover, notice that a system composed of a *class b* material rubbing against a *class a* material (such as mild steel and stainless steel) is thermally stable in the sense that the matching function is almost uniform, which implies that the capacity of heat removal remains almost constant with temperature elevation (compare the curves for Inconel and stainless steel to the curves for mild steel and sapphire).

6.3. Effect of the matching function on heat removal

To illustrate the influence of the matching function on the heat removed away from the surface, two materials were chosen: mild steel (*AISI 1020*) and stainless steel (*AISI 304-HN*). The characteristics of heat dissipation of each material are plotted in *figure 7*. Both materials were assumed to slide at 2 $m \cdot s^{-1}$ under a nominal load of 20 N under plastic contact conditions. The figure depicts the variation in the quantity of heat dissipated versus the ratio Θ/Θ_{max}. The quantity of heat dissipated was evaluated under the convenient assumption that all the heat generated at the interface is dissipated through a single asperity (not partitioned between the asperity pair). The radius of the asperity was calculated following the method of Lim and Ashby [10], and was found to be approximately 12 μm. Temperature gradients were evaluated at consecutive time increments, and then related to the instantaneous temperatures (and thereby to the ratio Θ/Θ_{max}). Two solutions are plotted in *figure 7*: the constant conductivity solution, which represents the amount of heat dissipated, calculated by evaluating the product of the temperature gradient and the room temperature thermal conductivity; and the variable conductivity solution, which represents the amount of heat dissipated, evaluated by means of a temperature-dependent conductivity.

It will be noticed that, individually, each material behaves as expected for its material class: the heat transfer rate predicted by the constant conductivity solution for mild steel (*class a* material, negative β coefficient) drops with temperature due to the effect of the negative matching function. Notice that the heat transfer rate drops further if the effects of the temperature on the thermal conductivity are accounted for. The opposite is noted for stainless steel (*class b* material, positive β coefficient). Therefore, it seems logical to expect that if mild steel were matched against stainless steel, the drop in the dissipation ability of mild steel would be compensated by the increase in the heat removal capacity of stainless steel.

Figure 8 depicts the variation in the rate of heat dissipation for two rubbing pairs. The first is a mild steel pair; the second is a mild steel–stainless steel pair. Conditions of sliding are the same as those of *figure 7*. The amount of heat shown in the figure is scaled with respect to the maximum heat removed by the mild steel pair. Note that for the same applied thermal load, the mild steel pair dissipates more heat than the mild steel–stainless steel pair. This is due to the value of the conductivity of mild steel, which is higher than that of stainless steel. The drop in the amount of heat conducted with time is due to the negative value of the effective matching function Γ_{eff} for each of the rubbing pairs (see *table III*). Note that as the room temperature conductivity of mild steel is almost three times that

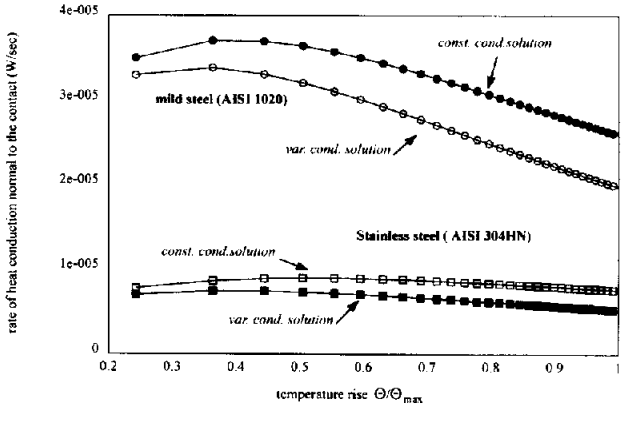

Figure 7. Variation in the rate of heat dissipation for mild steel (*AISI 1020*), and stainless steel (*AISI 304 HN*), with the non-dimensional temperature Θ/Θ_{max}. The rate of heat conduction is calculated by means of constant and variable conductivity solutions utilising the room and the temperature dependent thermal conductivities respectively.

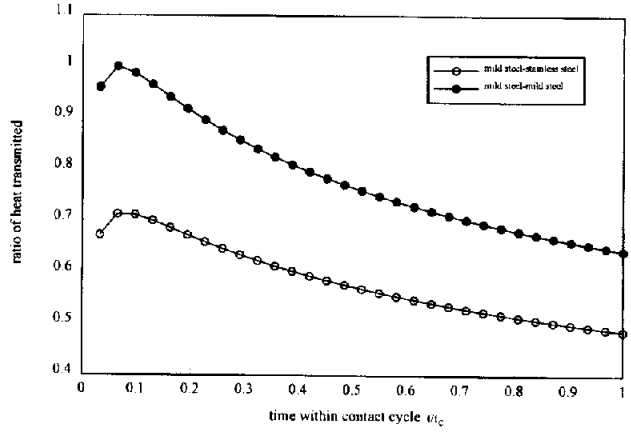

Figure 8. Comparison of the variation in the amount of heat removed by a mild steel asperity pair to that removed by a mild steel-stainless steel asperity pair with the non-dimensional contact time t/t_c.

TABLE III
Values of the effective matching function Γ_{eff} for several materials sliding against mild steel (*AISI 1020*). Load = 20 N, $U_{\text{slid}} = 2$ m·s^{-1}.

Material	$\alpha \times 10^{-5}$ (m^2·s^{-1})	β (K^{-1})	k_0 (W·m^{-1}·K^{-1})	Γ_{eff} (W·m^{-1}·K^{-1})
Sapphire[a]†	1.326	−0.00081	28.2	−13.9348
Tool steel (*AISI 52100*)[a]	0.956	−0.0004	35.4	−12.234
Stainless steel (*AISI 304 HN*)[b]	0.395	0.000874	13.8	−1.77
Zinc[c]	0.44	−0.000229	121.0	−20.86
Inconel[b]	0.31	0.002	9.133	2.6052
Mild steel (*AISI 1020*)[a]	0.79	−0.000486	51.823	−15.4308
Titanium[c]	0.932	−0.00017	21.9	−7.658

† superscript letters indicate material class.

of stainless steel (51.8 W·m^{-1}·K^{-1} for the former and 13.38 W·m^{-1}·K^{-1} for the later), mild steel will dominate the heat transfer process. This is so because the material with the higher conductivity carries a bigger portion of the dissipated heat. Consequently, the decrease in the conductivity of the mild steel will overtake the increase in the conductivity of stainless steel. This effect is better illustrated in *figure 9* which depicts the variation in the heat conducted away from the surface of contact with the ratio $\Theta/\Theta_{\max}$. Notice that the rate of decrease in the heat dissipation is almost identical for both curves. Again, this is due to the dominant influence of the mild steel asperity.

6.4. Effect of the matching function on the specific contact efficiency

Figure 10 is a plot of the specific dissipation efficiency, η_a, against the time of contact for the two

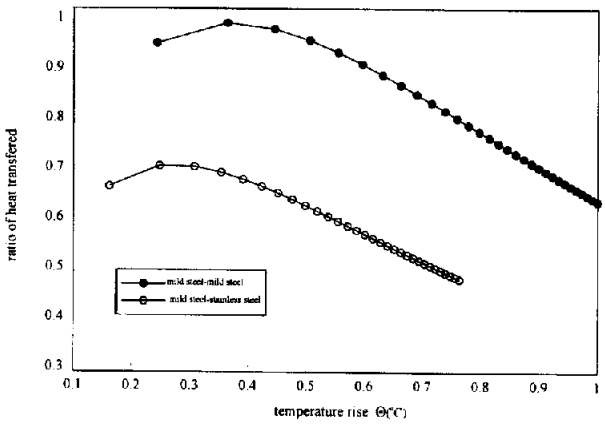

Figure 9. Comparison of the variation in the amount of heat removed by a mild steel asperity pair to that removed by a mild steel–stainless steel asperity pair with the non-dimensional temperature rise $\Theta/\Theta_{\max}$.

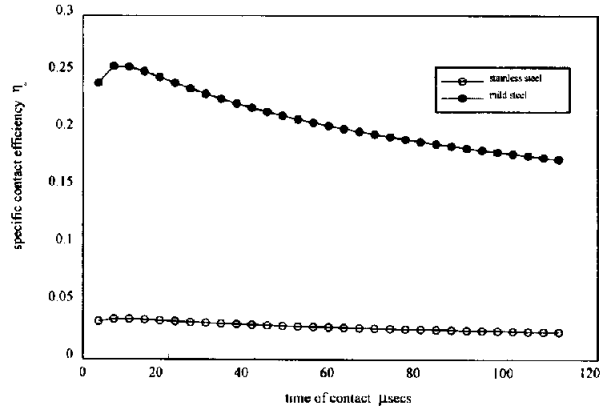

Figure 10. Variation in the specific contact efficiency η_a of the asperity pairs of *figure 8* with actual time of contact.

asperity pairs of *figures 8* and *9*. The nominal load and sliding speed are the same as those of the previous *figures*. Notice that, despite the increase in the amount of heat removed by the mild steel-stainless steel asperity pair, relative to that removed by the mild steel pair, the specific efficiency of the former is considerably smaller than the later. An interesting feature of the figure, however, is the change in η_a with respect to time, which is slower for the mild steel-stainless steel pair than that of the mild steel pair. This is due to the increase in the conductivity of stainless steel with temperature. Essentially the same effects can be observed in *figure 11* which traces the variation in η_a, with respect to temperature for the same asperity pairs.

The choice of the rubbing materials so as to achieve a positive matching function is always possible for *class b* rubbing pairs. The reason is that the Γ values for each material are inherently positive. The value of this parameter is, however, negative for *class a* materials due to the negative value of the β coefficient. This poses a challenging problem when either a *class a* material is to rub against a *class b* material, or when two *class a* materials rub against each other.

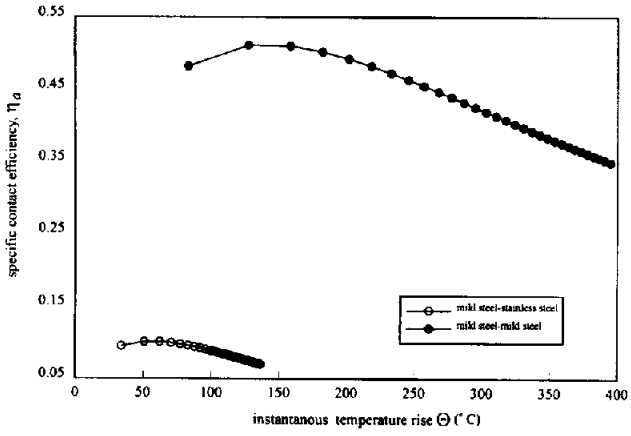

Figure 11. Variation in the specific contact efficiency η_a of the asperity pairs of *figure 8* with the instantaneous temperature rise at the centre of the contact spot.

In the first case, the situation is complicated if the conductivity at room temperature of the *class a* material is considerably higher than that of the *class b* material, with the former dominating the heat conduction process because it bears the biggest portion of the thermal load. Consequently, regardless of the improvement in heat removal conditions offered by the increasing conductivity of the *class b* material, the specific efficiency η_a of the asperity pair will drop. This applies to the example considered in this work, as the room temperature conductivity of mild steel is more than three times that of stainless steel (see *table II*).

In the case of *class a* rubbing pairs, the matching function is inherently negative due to the negative β coefficients. This case clearly poses a strong potential for accelerated thermal-induced failure as the drop in the conductivity may induce an accumulation of frictional heat in the contact and the sub-contact layers. In essence, the control of the heat dissipation away from the surface, so as to minimise thermal damage, has to be attempted through the control of the parameter Γ, i.e. by increasing the positive slope of the heat penetration coefficient with temperature.

6.5. Effect of a thin layer on the matching function

Recalling equation (18a and b), we may conceive that the control of the parameter Γ may be achieved through either magnifying the product βk_0 or minimising the effect of the diffusivity. The objective in the first option is to stabilise the variation in the conductivity with temperature. That is, minimisation of a negative β coefficient or maximisation of a positive β coefficient. The objective in the second option is to obtain a lower effective diffusivity. The difficulty here is the coupling between the conductivity and the diffusivity of the same material: in general, high thermal conductors possess also high thermal diffusivity [11]. Perhaps an effective solution is the application of a thin coating to the thermally dominant material [12]. In this way, the individual Γ values would now represent a resultant value, combining that of the material and the coating. If the coating slightly reduces the thermal conductivity of the dominating material, but compensates for the negative β coefficient, then equal thermal load sharing would be realised. Consequently, the chance of neutralising the destructive effect of the latter is greatly enhanced.

To examine the above hypothesis, a set of calculations was performed for the same rubbing pairs introduced above, but taking into account the presence of a 10 μm thin layer of Inconel on one of the mild steel asperities. *Table IV* summarises the changes in the matching function due to the presence of the Inconel layer. Note that the application of the layer causes the effective room temperature conductivity to decrease: from 51.8 $W \cdot m^{-1} \cdot K^{-1}$ for mild steel to around 26 $W \cdot m^{-1} \cdot K^{-1}$ for the layer and the substrate. This is accompanied by a positive change in the effective β coefficient from about −0.000486 for the former, to around 0.000759 for the latter. In this manner, a drop in the matching function at higher temperature gradients is largely avoided. This is apparent in *figure 12*, which compares the behaviour of the matching function for both rubbing pairs with and without the deposited layer. Notice that the presence of the layer significantly enhances heat removal for the mild steel pair, especially at higher temperatures.

The improvement in heat removal, however, may be achieved at the expense of the room temperature conductivity. This was seen in the present case, where the room temperature conductivity dropped by almost an order of magnitude. This may lead to an initial drop in the amount of heat transferred in the beginning of the contact cycle, as compared to the case where no layer is deposited. However, with time progression the temperature rise will increase, and the matching function will be dominant, with the effect that the efficiency of heat removal will be enhanced due to the positive β coefficient. The result will be that the *total*

TABLE IV
Comparison of the values of the effective matching function Γ_{eff} for a mild steel, and a mild steel-stainless steel rubbing pair, with and without a 10 μm thin layer applied to the mild steel asperity.

Γ_{eff} ($W \cdot m^{-2} \cdot K^{-1}$)	with 10 μm Inconel layer	without layer
Mild steel–mild steel	−2.933	−15.4308
Mild steel–stainless steel	5.5185	−1.77

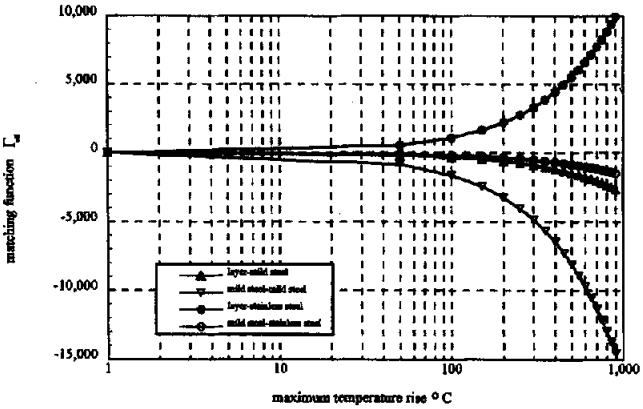

Figure 12. Effect of applying a thin coating on the behaviour of the matching function Γ_{eff} for the asperity pairs of *figure 8*, with temperature. Two cases are compared: both metals rubbing without the layer, and the effect of a 10 mm thick Inconel layer applied to mild steel. Load = 20 N, and $U_{\text{slid}} = 2\ \text{m}\cdot\text{s}^{-1}$.

amount of heat conducted throughout the contact cycle would be higher in the presence of a layer than the amount for mild steel by itself. This may be verified by comparing the values (in *figure 12*) of the matching function for mild steel with and without a layer, especially at higher temperature rises (above 200 °C).

7. SUMMARY AND CONCLUSIONS

The change in the thermal properties of rubbing materials with temperature influences frictional heat removal. The temperature rise induces variation in the so-called 'coefficient of heat penetration'. This variation was termed the matching function of a material. The sign of the effective matching function, that of the rubbing pair, was identified as an indicator of the nature of heat removal in a contact cycle.

The sign of the matching function follows closely the sign of the temperature coefficient of thermal conductivity β of the material. For *class a* materials (negative β coefficient), the matching function assumes a negative sign. This implies a drop in the rate of heat removal with temperature increase. By contrast, the matching function in case of *class b* rubbing pairs assumes a positive sign. This implies an increase in the rate of heat removal with temperature increase. An interesting case arises when a *class a* material slides against a *class b* material. In such an event, the material with both a higher room temperature conductivity and a higher product βk_0 will dominate heat removal.

A criterion for the thermal compatibility of rubbing materials is also proposed. This criterion requires the choice of materials for rubbing applications to be made so as to maintain, in order of preference, a positive, zero, or slightly negative matching function. Subsequently this criterion was used as a guide to enhance the heat transfer between a rubbing steel pair by applying a tribological thin coating to the dominant material.

It is recognised that other parameters such as strength, toughness, hardness, and tribological compatibility, play a key role in the selection of suitable materials for rubbing applications. While thermal compatibility may not dominate, it is envisaged that a comprehensive thermal compatibility map will provide some additional criteria for reducing the bewildering range of available materials.

REFERENCES

[1] Rozeanu L., Pnueli D., Two temperature gradients model for friction failure, J. Tribol.-T. ASME 100 (1978) 479–485.

[2] Carslaw H.S., Jaeger J.C., Conduction of heat in solids, Oxford University Press, London, 1959.

[3] Grigull U., Sandner H., Heat Conduction, International Series in Heat and Mass Transfer, Hemisphere, New York, 1984.

[4] Bhushan B., Magnetic head-media interface temperatures. Part 1: analysis, J. Tribol.-T. ASME 109 (1987) 243–251.

[5] Dundurs J., Panek C., Heat conduction between bodies with wavy surfaces, Int. J. Heat Mass Tran. 19 (1976) 731–736.

[6] Cowan S.R., Winer W.O., Frictional heating calculations, in: Blau P.J. (Ed.), Friction, lubrication and wear technology, ASM Handbook, vol. 18, Metals Park, Ohio, 1993, pp. 39–44.

[7] Archard J.F., The temperatures of rubbing surfaces, Wear 2 (1959) 438–455.

[8] Abdel-Aal H.A., Error bounds of variable conductivity temperature estimates in frictionally heated contacts, Int. Commun. Heat Mass 25 (1) (1998) 99–108.

[9] Abdel-Aal H.A., Smith S.T., On friction-induced temperatures of rubbing metallic pairs with temperature dependant thermal properties, Wear 216 (1998) 41–59.

[10] Lim S.C., Ashby M.F., Wear mechanism maps, Acta Metall. Mater. 35 (1) (1987) 1–24.

[11] Touloukian Y.S., Powell R.W., Ho C.Y., Nicolaou M.C., Thermal Diffusivity, Plenum Press, New York, 1973.

[12] Antonetti V.W., Yovanovich M.M., Enhancement of thermal contact conductance by metallic coatings: theory and experiment, J. Heat Trans.-T. ASME 107 (1985) 513–519.

[13] Özişik M., Necati, Boundary value problems of heat conduction, Dover Publications, New York, 1989.

[14] Anderson D.A., Tannehill J.C., Pletcher H.R., Computational Fluid Mechanics and Heat transfer, McGraw Hill, New York, 1984.

[15] Post D., Wood J.D., Determination of thermal strains by Moire' interferometry, Exp. Mech. 29 (1989) 318–322

[16] Moslehy F.A., Seif M.A., Rice S.L., Measurement of surface displacements in a tribological contact, Exp. Mech. 30 (1990) 49–55.

[17] Storm M.L., Heat conduction in simple metals, Thesis, New York University, New York, USA, 1950.

[18] Ling, F.F., Rice J.C., Surface temperatures with temperature-dependant thermal properties, ASLE Trans. 9 (1966) 195–201.

[19] Abdel-Aal H.A., A remark on the flash temperature theory, Int. Commun. Heat Mass 24 (2) (1997) 241–250.

APPENDIX A

Finite difference derivation of the model equation

The total amount of heat flowing away from the contact spot into a solid is given by [13] as:

$$\underset{t_1-t_2}{Q}\int_{t_1}^{t_2}\Big[\int_A k\,\frac{\partial T}{\partial \eta}\,(\vec{r},t)\,\mathrm{d}A\Big]\mathrm{d}t \qquad \text{(A-1)}$$

where $\partial/\partial\eta$ denotes differentiation along the outwards-drawn normal unit vector to the boundary surface element $\mathrm{d}A$, and $\vec{r}$ is the position vector. For 1-D heat flow and a nominally flat contact spot in the X–Y plane, equation (1) may be written as:

$$\underset{t_1-t_2}{Q}\int_{t_1}^{t_2}\Big[\int_A k\,\frac{\partial T}{\partial Z}(z,t)\,\mathrm{d}A\Big|_{z=0}\Big]\mathrm{d}t \qquad \text{(A-2)}$$

Computing the inner integral, equation (2) takes the form:

$$\underset{t_1-t_2}{Q}\int_{t_1}^{t_2} k\,\frac{\partial T}{\partial Z}(z,t)\Big|_{z=0} A_c\,\mathrm{d}t \qquad \text{(A-3)}$$

To trace the rate of heat flow through the contact at infinitesimal time increments, we express equation (3) in a finite difference form as in [14]:

$$\underset{t\to t+\Delta t}{\frac{\Delta Q}{}} = -A_c\int_{t_0}^{t_0+\Delta t} k\Big\{\frac{T(Z_0+\Delta Z,t)-T(Z_0,t)}{\Delta Z}\Big\}\Big|_{Z=0}\mathrm{d}t \qquad \text{(A-4)}$$

Invoking the mean value theorem, equation (4) may be integrated as:

$$\frac{\Delta Q}{\Delta t} = -Ak\Big\{\frac{T(Z_0+\Delta Z,t_0+\Delta t)-T(Z_0,t_0+\Delta t)}{\Delta Z}\Big\}\Big|_{Z=0} \qquad \text{(A-5)}$$

Summing the heat penetrating through the surface $Z=0$ into each of the rubbing solids we may write:

$$\dot{q}_i = -A_c\Big[k_1\Big\{\frac{\Theta(\Delta Z,t_i)-\Theta(0,t_i)}{\Delta Z}\Big\}_1 + k_2\Big\{\frac{\Theta(\Delta Z,t_i)-\Theta(0,t_i)}{\Delta Z}\Big\}_2\Big] \qquad \text{(A-6)}$$

where Θ denotes the temperature rise above the initial temperature $T(Z,t_0)$. Finally upon expressing the thermal conductivity of each solid in the linear form $k(\Theta) = k_0(1+\beta\Theta)$, we may express the rate of heat penetrating the contact spot towards the bulk of the asperities as:

$$\dot{q}_i = -A_c\Big[k_{0_1}[1+\beta_1\,\theta(0,t_i)]\Big\{\frac{\Theta(\Delta Z,t_i)-\Theta(0,t_i)}{\Delta Z}\Big\}_1 + k_{0_2}[1+\beta_2\,\theta(0,t_i)]\Big\{\frac{\Theta(\Delta Z,t_i)-\Theta(0,t_i)}{\Delta Z}\Big\}_2\Big] \qquad \text{(A-7)}$$

Equation (A-7) is identical to equation (3) in the main text except that the dependence of the temperature rise on time was omitted for convenience.

Note that the temperature gradient underneath the asperity is, in essence, non-linear. This may be remedied in the current formulation by the proper choice of the diffusion length ΔZ [10]. For this reason we choose the diffusion length so as to yield the actual value of the gradient at the point of interest along the axis of the asperity.

Accuracy range for the model equation (3)

The idea implied in the derivation of equation (3) in the main text is to express the temperature gradients in both rubbing members in terms of instantaneous quantities. That is, to trace the evolution of the temperature gradients on both sides of the contact spot (and thereby the quantity of heat dissipated towards the bulk of the material) at infinitesimal time increments t_i within the contact cycle. This is achieved by calculating an instantaneous temperature difference $[\Theta_s - \Theta_b]^{(t_i)}$ and a maximum instantaneous penetration depth $Z_{p_{max}}(t_i)$. Through the substitution of these instantaneous quantities in a finite-difference formulation of the Fourier equation, the heat dissipated away from the contact spot is expressed as a rate (heat flow per unit time). This allows for *freezing* the time parameter, or in optical terms, allows for the frame-by-frame study of the gradients and the quantity of heat transferred. Such an idea is frequently invoked in the optical measurements of the instantaneous displacement fields [15]. Naturally, one may question the domain of validity of such an approach. Indeed, this approach is valid only for very small times (order of 10–100 μs), a time domain which includes the duration of contact between the micro roughness for practical nominal loads and sliding speeds [16].

To enhance the accuracy of the calculations, two points have to be addressed. Firstly, what is the relation between the time step (t_i) and the depth of penetration ΔZ (or $Z_{p_{max}}$), and, secondly, what is the criterion by which this penetration depth will be judged small so as to allow for the negligence of the storage term:

$$\frac{1}{\Delta t}\int_{t_0}^{t_0+\Delta t}\int_0^{Z_p}\rho C\,\frac{\partial T}{\partial t}(z,t)\,\mathrm{d}t \qquad \text{(A-8)}$$

The first question may be answered by appealing to the well-known Von Neumann–Courant stability criterion. For the finite-difference formulation of the 1-D equation the critical size of the co-ordinate step ΔZ is related to the time step by:

$$\Delta Z \leq \sqrt{2\,\alpha\,t} \tag{A-9}$$

where α is the thermal diffusivity of the material. Satisfying equation (A-9) ensures that the errors in the temperatures are minimal.

To address the second question (which is more critical to the model equation), we first note that the semi-infinite body solution was used to evaluate the maximum penetration depth, that is, the depth of the so-called thermal layer Z_{Pmax}. In this formulation, the time-dependent quantity of heat conducted away from the surface is written as in [13]:

$$q(t) - k\,\frac{\partial T}{\partial Z}(Z,t)\Big|_{z=0} = C\,k\,\frac{(T_0 - T_\mathrm{i})}{\sqrt{\alpha\,t}} \tag{A-10}$$

where C is a constant almost equal to $\pi^{-1/2}$, and depending on whether the type of solution is approximate or exact, and T_i is the initial temperature at the surface $Z = 0$. The maximum penetration depth that may be used to calculate the quantity of heat without the storage term is equal to $2\,\{\alpha\,t\}^{1/2}$.

Now, if one assumes first that the asperity was initially at a uniform temperature T_i, and one adopts the definition of the 'thickness of the thermal layer' as the thickness beyond which, for practical purposes, there is no heat flow (and consequently no temperature rise above the initial temperature), then one may write:

$$q(t) = \sum_j -k_j\,\frac{\partial T}{\partial Z}(Z,t_\mathrm{i})\Big|_{z=0} = \sum_{j=1}^{j-2} -k_j \left\{ \frac{[T_0 - T(Z \geq Z_{\mathrm{Pmax}})]}{2\sqrt{\alpha_j\,\bar{t}}} \right\}^{t_\mathrm{i}} \tag{A-11}$$

This equation is identical to equation (3), which starts the analysis, except that the latter was derived from a finite-difference-based formulation.

APPENDIX B

Combining the thermal properties of the layer and the substrate

To determine the value of matching function when a thin coating is applied to one of the contacting surfaces, the equivalent thermal properties and their respective variation with temperature have to be evaluated. In this appendix we derive the expressions used to compute such equivalent quantities.

B.1. Calculation of the equivalent diffusivity α_{eq}

The thickness of the applied coating (layer), δ_l, which is known a priori, represents the distance that must be travelled by a temperature pulse originating at the asperity tip to reach the substrate material. Upon penetrating the thickness of the layer, the strength of the original pulse has decayed to some new value. So the problem reduces to the computation of two quantities: the first is the strength of the temperature pulse after it penetrates the layer (i.e. at the interface between the layer and the substrate). Once this quantity is found, we proceed to calculate the penetration depth of the new pulse into the substrate. That is, to calculate Z_{Pmax} for the substrate material under the influence of the reduced temperature pulse. This would be represented by the distance which is covered until this new pulse Θ_s, decays to the 1 % criterion developed in section 4.

Applying equation (11) we may write:

$$\xi_\mathrm{l} = \frac{\delta_\mathrm{l}}{2\sqrt{\alpha_\mathrm{l}\,t_\mathrm{i}}} \tag{B-1}$$

Substituting equation (B-1) in equation (10), the strength of the pulse at the interface between the substrate and the layer is then given by:

$$\overline{\Theta}_{\mathrm{L/S}} = \mathrm{erfc}(\xi_\mathrm{l}) \tag{B-2}$$

recalling the definition of the parameter $\overline{\Theta}$, we may write the actual strength of the temperature pulse at the interface as:

$$\Theta_{\mathrm{L/S}}(t) = \overline{\Theta}_{\mathrm{L/S}}\,\Theta_0(t) \tag{B-3}$$

Using the results of equation (B-3) we may calculate the penetration depth into the substrate due to a pulse of strength $\Theta_{\mathrm{L/S}}(t)$ operating at the interface. Thus we obtain from equation (13):

$$\delta_\mathrm{s} = Z_{0.01_{\Theta_{\mathrm{L/S}}}} = 2\,\xi_\mathrm{s}\sqrt{\alpha_\mathrm{s}\,t_\mathrm{i}} \tag{B-4}$$

where

$$\mathrm{erfc}(\xi_\mathrm{s}) = \overline{\Theta}_\mathrm{s}$$

Now, the total penetration depth into the layer–substrate has to equal the penetration depth that would have been calculated based on an equivalent diffusivity α_{eq}:

$$\delta_{\mathrm{tot}} = \delta_\mathrm{l} + \delta_\mathrm{S} = Z_{0.01_{\mathrm{eq}}} \tag{B-5}$$

Equation (B-6) may be written as:

$$\delta_{\mathrm{tot}} = 4\sqrt{\alpha_{\mathrm{eq}}\,t_\mathrm{i}} \tag{B-6}$$

from which the equivalent diffusivity α_{eq} is evaluated. By repeating the same procedure using the value of the diffusivities of the layer material and of

the substrate material at different temperatures, a corresponding array containing the variation of the substrate penetration depths with temperature, $\delta_s(\Theta)$, is obtained. This may be then used to calculate the equivalent thermal conductivity of the layer substrate combination.

B.2. Calculation of the equivalent conductivity k_{eq}

Assuming perfect contact between the layer and the substrate, the equivalent conductivity may be calculated as in [3]:

$$k_{eq} = \frac{\delta_l + \delta_s}{\delta_l/k_l + \delta_s/k_s} \tag{B-7}$$

Substituting the value of $\delta_s(\Theta)$, the equivalent conductivity as a function of temperature is written as:

$$k_{eq}(\Theta) = \frac{\delta_l}{k_l(\Theta)} + \frac{\delta_s}{k_s}(\Theta) \tag{B-8}$$

Equation (B-8) yields the value of the equivalent conductivity at discrete temperatures. This in turn may be modelled in the linear form:

$$k_{eq}(\Theta) = k_{0_{eq}}[1 + \beta_{eq}\,\Theta] \tag{B-9}$$

Equation (B-9) was used to calculate the equivalent temperature coefficient of conductivity β_{eq}, and to predict the variation of the equivalent thermal conductivity for the layer–substrate combination. The results are depicted in figure B-1, where the conductivity of mild steel (*AISI 1020*) and Inconel (*X-70*) are plotted along with the equivalent conductivity for a 10 mm thick layer of Inconel applied to mild steel both at discrete temperatures and as modelled by equation (B-9).

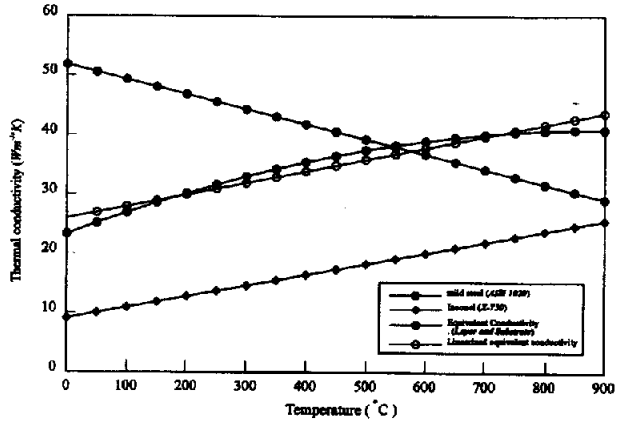

Figure 13. Variation of the effective thermal conductivity of the combination of the Inconel layer and the substrate with temperature.

APPENDIX C

C.1. Effect of the variation in the thermal conductivity on the penetration depth $Z_{p_{max}}$

Equation (10) is the solution of a linear constant conductivity problem. To obtain the solution of the same problem when the conductivity varies with temperature, we invoke the so-called *Kirchoff transformation* [13] which is applied as follows.

Assume that the thermal conductivity varies linearly with temperature, i.e.:

$$k(T) = k_0(1 + \beta T) \tag{C-1}$$

Define a new variable, U, such that:

$$U = \frac{1}{k_0}\int_{T_0}^{T} k(T)\,dT \tag{C-2}$$

Substituting this new variable in the heat equation, we obtain an equation that is identical to the original heat equation, except that the solution now will yield the solution in terms of the transformed variable U (equivalent to Θ in equation (10) of the main text).

To obtain the variable conductivity solution, we apply to equation (10) the inverse transformation:

$$T = \frac{1}{\beta}\left\{\sqrt{1 + 2\beta U} - 1\right\} \tag{C-3}$$

and we obtain:

$$T = \frac{1}{\beta}\left\{\sqrt{1 + 2\beta\overline{\Theta}} - 1\right\} \tag{C-4}$$

where Θ is the solution of the linear constant conductivity problem and T is the solution of the variable conductivity problem.

Now since $0 \le \Theta \le 1$, it follows that the maximum error in the estimate of the penetration depth introduced by neglecting the variation in the conductivity with respect to temperature is encountered when $\Theta = 1$. Hence the maximum error, φ_{max}, may be defined as the ratio of the actual to the constant conductivity temperatures when $\Theta = 1$, i.e.:

$$\varphi_{max} = \frac{T}{\overline{\Theta}} = \frac{1}{\beta}\left\{\sqrt{1 + 2\beta} - 1\right\} \tag{C-5}$$

substituting the value of β for the materials used (from *table III*) in equation (C-5), the maximum error is readily obtained.

Table V gives the value of the maximum error for the materials used in the current investigation calculated by means of equation (C-5). It will be noticed that this error is quite insignificant. This is not surprising,

as the penetration depth is an explicit function of the diffusivity (and not the conductivity).

C.2. Effect of the variation in the thermal effusivity with temperature

There are two quantities that contribute to the value of the effusivity: the thermal conductivity, and the thermal capacity (product of the density and the specific heat). For metals, the specific heat increases with temperature elevation, whereas the density decreases slightly (by a factor of $5{\cdot}10^{-5}$ °C^{-1} [17]) with temperature. The change in the conductivity, however, is two to three times the corresponding change in the diffusivity. For example, the change in the diffusivity of Duralumin at 600 °C is approximately −4 % of that at room temperature, while the corresponding change in conductivity is approximately 13 % of that at room temperature. Essentially, the same applies to steels, where the change in the diffusivity at 900 °C (for example) compared to the room temperature value is almost one third of the corresponding change in conductivity [22]. So the change in the thermal capacity tends to somewhat offset the effect of the variation in the conductivity with temperature. As such, the dominant thermal influence at the interface, surface $Z = 0$, is the thermal conductivity, as explicated in the work of Storm [17] and Ling and Rice [18], Abdel-Aal [8, 19] and Abdel-Aal and Smith [9]. *Table VI* summarises the value of the effusivity for the materials used in the current investigation at both room temperature and at 1 200 °K. It will be noticed that the variation in the effusivity at this high temperature is still fairly moderate, so that at practical temperatures typical of sliding systems, this variation may be considered insignificant.

TABLE V
Maximum error introduced by neglecting the variation in the conductivity in the calculation of the penetration depth of a temperature pulse.

Material	β (°C)	$\overline{\Theta}$	φ
Sapphire	−0.00081	1.00041	−0.0041
Tool steel (*AISIn 52100*)	−0.0004	1.0002	−0.0002
Stainless steel (*AISI 304 HN*)	0.000874	0.9995	0.000437
Zinc	−0.00023	1.000115	−0.00011
Inconel	0.002	0.999	0.0001
Mild steel (*AISI 1020*)	−0.00049	1.0002	−0.00024
Titanium	−0.00017	1.000085	$-8.5{\cdot}10^{-5}$

TABLE VI
The effusivity of the materials used in the current work at room temperature and at 1 000 °K.

Material	Ω (293 °K)	Ω (1 200 °K)	$\omega^{\dagger}$
Sapphire	9 223	8 301.2445	0.9
Tool Steel (*AISI 52100*)	13 507.92	14 121.74	1.045
Stainless Steel (*AISI 304 HN*)	7 493.175	10 748.02	1.434
Zinc	18 237.79	17 540.72	0.962
Inconel	6 761.144	11 270.67	1.66
Mild steel (*AISI 1020*)	13 835.22	13 980.7	1.01
Titanium	7 172.385	7 728.676	1.078

† $\omega = \Omega$ (1 200 ° K)/Ω (293 °K).